Application of hybrid cement in passive fire protection of steel structures

Jakub Šejna

Department of Steel and Timber Structures, Czech Technical University in Prague, Prague, Czech Republic

Stanislav Šulc and Vít Šmilauer

Department of Mechanics, Czech Technical University in Prague, Prague, Czech Republic

Pavel Reiterman

Experimental Centre, Czech Technical University in Prague, Prague, Czech Republic, and

František Wald

Department of Steel and Timber Structures, Czech Technical University in Prague, Prague, Czech Republic

Abstract

Purpose – The aim of this paper is to determine the thermal conductivity of a protective layer of alkali-activated cement and the possibility of performing fire protection with fireclay sand and Lightweight mortar. Unprotected steel structures have generally low fire resistance and require surface protection. The design of passive protection of a steel element must consider the service life of the structure and the possible need to replace the fire protection layer. Currently, conventional passive protection options include intumescent coatings, which are subject to frequent inspection and renewal, gypsum and cement-based fire coatings and gypsum and cement board fire protection.

Design/methodology/approach – Alkali-activated cements provide an alternative to traditional Portland clinker-based materials for specific areas. This paper presents the properties of hybrid cement, its manufacturability for conventional mortars and the development of passive fire protection. Fire experiments were conducted with mortar with alkali-activated and fireclay sand and lightweight mortar with alkali-activated cement and expanded perlite. Fire experiment FE modelling.

Findings – The temperatures of the protected steel and the formation of cracks in the protective layer were investigated. Based on the experiments, the thermal conductivities of the two protective layers were determined. Conclusions are presented on the applicability of alkaline-activated cement mortars and the possibilities of applicability for the protection of steel structures. The functionality of the passive fire layer was confirmed and the strengths of the mortar used were determined. The use of alkali-activated cements was shown to be a suitable option for sustainable passive fire protection of steel structures.

Originality/value – Eco-friendly fire protection based on hybrid alkali-activated cement of steel members.

Keywords Fire protection, Alkali-activated cement, Hybrid cement, Modelling, Material properties

Paper type Research paper

1. Introduction

Fire safety is one of the most important topics of investigation and assessment in the field of construction (Babrauskas, 2005; Wang *et al.*, 2013; Buchanan and Abu, 2017). The most

problematic task in the design of a building is often how to take a comprehensive approach to assessing the fire resistance of the whole structure or of a detail, which can significantly reduce the overall fire safety of the building. The design of the building into fire compartments that ensure the safe evacuation of people, animals and property or the assessment of fire water supply, access roads and escape corridors for firefighters with the static design are basic procedures in fire design. New materials used for room equipment and increased electricity consumption have placed increased demands on the approach to fire protection design (Lennon and Moore, 2003; Mizukami and Tanaka, 2017; Ozaki *et al.*, 2018). Nowadays, it is common to include, for example, the heat released from plastics in the development of fires, which are increasing in number and are often the source of fire. Structures are more heated in this aspect than they were in previous decades. The stresses placed on building structures in recent decades have increased the number of combustible objects in the compartment and therefore the quantities of combustible substances released into the surrounding environment (Nan *et al.*, 2022; Rangwala and Raghavan, 2022).

Steel structures are the most affected by these changes. Steel members experience a rapid reduction in yield strength as a result of increased temperatures. The assessment of a steel member depends, for example, on the determination of the critical temperature of the member. The basic options for protecting a steel element from the effects of fire include cladding with board materials (gypsum board, cement board, etc.), fire coatings, fire spraying or water sprinkling for cooling. As an example, a problem with fire coatings is that they are a laborious solution. Since they have limited durability, the cost of renewal becomes high. Currently, there is an increased focus on the sustainability of buildings, and therefore, it is necessary to find new solutions or develop new materials to reduce the environmental impact (Siebers *et al.*, 2017; Kim and Kim, 2020; Mirshekarlou *et al.*, 2021).

It is possible to partially protect steel structures. In this case, higher deflection of the beams is allowed when the column and joints are protected. This method results in a possible membrane effect on the floor slab and provides the load-bearing capacity of the connection. This procedure was discussed in more detail by Šejna *et al.* (2023a, b), who summarized the possibilities of partial passive protection and its design. An option for partial fire protection or protection of the whole steel member is the use of spraying or concreting with mixtures of lightweight concrete or concrete with fire-resistant aggregate filler. In terms of the durability of building structures, the use of alternative cements that have lower CO_2 emissions or the use of recycled alkali-activated concrete is possible. The use of alkali-activated cements is a well-known concept. However, in terms of applicability, new alkaline-activated cements with different properties and lower CO_2 emissions during their production than their predecessors are constantly being developed.

The traditional solution to protecting steel is to create a layer of thermal insulation material. Most cementitious materials do not behave well when exposed to high temperatures due to high-temperature gradients followed by thermal expansion and contraction during drying. The resulting cracks cause increased heat transfer to the structure and loss of integrity.

The possibility of using alternative cements and different variations of dispersed reinforcement was investigated in research conducted by Jogl *et al.* (2016a, b), where the use of fireclay sand or other insulating fillers was investigated for the development of refractory concrete. Factors that affect the workability of the mixes were investigated in terms of the volume of water required to mix with the insulating fillers or cements used. The knowledge gained from successive tests of the samples in terms of mechanical properties and fire resistance could be used in the design of a protective layer of hybrid alkali-activated cement with a lightweight filler to increase fire resistance.

Preliminary results (Daxner, 2016) have demonstrated the superior resistance of lightweight mortars made from alkali-activated cement when compared to mortars made of equivalent gypsum binder or aluminate cements. Pilot tests for a larger experiment were carried out on a laboratory burner (Šulc *et al.*, 2021).

Alkali-activated cements bring advantage in generally lower chemically-bound water in reaction products, therefore fire exposure should be less detrimental to conventional materials (Shi *et al.*, 2006). This paper tests a hybrid cement, called H-cement, which is composed of 20% Portland clinker, fly ash, and granulated blast furnace slag, activated with sodium sulphate. The production of H-cement reduces CO_2 emissions by 80% in comparison with the production of OPC (Hlaváček *et al.*, 2015; Daxner, 2016; Martauz *et al.*, 2016).

At high temperatures, H-cement exhibits ceramic-like properties. When H-cement is heated to high temperatures, the melting phases of crystalline aluminosilicate are converted to a ceramic form at temperatures above 800°C, so no significant crack development occurs. The transformation and the contained geopolymer water are endothermic materials that are very resistant to the effects of fire. The design of the protective concrete layer of an H-cement over steel element takes advantage of the low heat transfer. The thermal conductivity of the H-cement concrete layer using expanded perlite as a filler is in the range of 0.1–0.3 W/(m·K) (Daxner, 2016).

From the sustainable point of view of buildings and reduction of CO_2 emissions, alkali-activated cements appear to be an excellent option. For example, alkali-activated cements can be produced with the use of recycled concrete (Damrongwiriyanupap *et al.*, 2022). Hydrated hybrid cements (H-cements) have specific properties that other cementitious materials lack (Wang *et al.*, 2022). H-cements are predicted to have a high level of adhesion to a cleaned steel surface, which means that substrate preparations for construction can be the same as for coatings and sprays. The significant utility properties of hybrid cement include the pozzolanic reaction of fly ash, the latent hydraulic reaction of slag and the alkaline activation of the inorganic geopolymer. A low final price of H-cement is achieved by using a low percentage by weight of Portland clinker (Jani and Imqam, 2021). H-cement also contains a low percentage of SiO_2, CaO, SO_3 and Na_2O, see Table 1 (Martauz *et al.*, 2016).

In the development of H-cement, substances with negative properties for the durability of a building or with a negative impact on the environment were eliminated. Mixed mortar with w/b = 0.4 has properties such as strength class 32.5 R compared to the properties of conventional Portland cement mortar of class 42.5 R with w/b = 0.5 (Martauz *et al.*, 2016).

To investigate the effect of the protective layer on increasing the fire resistance of steel structures, a formulation was developed for the applicability of H-cement as a binder in combination with fireclay sand. The aim of developing the mixture was to reduce the water content and to limit the use of additives, such as plasticizers. Martauz has published a comparison between H-cement mortars and OPC with partial strengths by Martauz *et al.* (2016). Table 2 presents the values for H-cement and for CEM I 42.5 R for a comparison. H-cement shows greater brittleness with lower hydration heat than conventional OPC at 28-day strength. H-cement can be used in the same cases as low-hydration heat cements (Martauz *et al.*, 2016).

SiO_2	40.0%
CaO	20.0%
SO_3	3.0%
Na_2O	2.0%
Source(s): Martauz *et al.* (2016)	

Table 1.
Minimum oxides in
H-cement

The adhesive properties of the H-cement paste and H-cement concrete with fireclay sand were tested for the behavioural properties of the proposed mix. At the same time, experiments were also conducted in a fire furnace to investigate the effect of adhesion to the concrete untreated surface. The results showed the possibility of using lightweight concrete or concrete with H-cement fireclay sand for fire protection of steel and concrete structures (Šejna *et al.*, 2023a).

In this paper, additional experiments are presented to confirm the behavior of the H-cement fire protection layer of steel structures. Based on the experiments, the material properties of lightweight concrete and concrete with H-cement sand as a function of temperature were determined.

2. Sample preparation

Additional experiments were carried out based on the previous experiments performed by Šulc *et al.* (2022) and Šejna *et al.* (2023a, b) to determine the possible thermal properties of the H-cement, fire protection layer. In the basic research, the samples were tested with a laboratory Bunsen burner, the production of samples for the tests in the small-scale furnace is presented below.

2.1 H-cement mortar from fireclay sand

Mortar with H-cement and fireclay sand was subjected to mixability tests according to a modified recipe based on knowledge from the development of refractory concretes (Jogl *et al.*, 2016a, b). The modified mixture for the use of H-cement is presented in Table 3. The PVA fibres, 12 mm long, serve mainly to decrease vapor pressure in a fire test.

During the investigation of the workability of the modified original mixture, it was necessary to supply additional water during mixing in the machine. The plasticizer, which was originally set at 1.8%, was not adequate for a mixture. The water/binder ratio was,

Parameter	Unit	H-cement	CEM I 42.5 R
Standard consistency	%	32 ± 2.0	29.1 ± 1.8
2-day compressive strength	MPa	17.5 ± 3.0 (w/c = 0.4)	33.7 ± 2.0 (w/c = 0.5)
28-day compressive strength	MPa	36.5 ± 4.0 (w/c = 0.4)	59.2 ± 1.6 (w/c = 0.5)
90-day compressive strength	MPa	41.5 ± 3.0 (w/c = 0.4)	63.1 ± 1.9 (w/c = 0.5)
2-day flexular strength	MPa	3.5 ± 0.5 (w/c = 0.4)	6.4 ± 0.4 (w/c = 0.5)
28-day flexular strength	MPa	4.4 ± 0.4 (w/c = 0.4)	8.9 ± 0.4 (w/c = 0.5)
90-day flexular strength	MPa	9.0 ± 0.3 (w/c = 0.4)	9.3 ± 0.3 (w/c = 0.5)
Hydrating heat	J/g	185	359
Source(s): Martauz *et al.* (2016)			

Table 2.
Characteristic strengths of H-cement and CEM I 42.5 R

	Specifications	Weight [kg]
H-cement	–	464
water	–	172
Fre clay sand	0–1 mm	4,642
	1–2 mm	929
PVA fibres	12 mm	1.20
Source(s): Author's own creation		

Table 3.
Mixture for H-cement mortar with fireclay sand for 1 m³

therefore, gradually adjusted and the plasticizer for the heavy mortar was omitted (first step: increasing the water/binder ratio to 0.30).

However, after this treatment, the mixture was very dense and insufficiently compact. The two mixtures were tested, and the water coefficient (w/b) was increased from 0.30 to 0.40. These changes were made to determine the consumption of water required to hydrate the H-cement, see Figure 1. In the case of using a plasticizer, it would be possible to reduce the ratio w/b.

The properties of the mixture are close to those of conventional concrete (density = 2030 kg/m^3), but the mix retains its positive properties due to the use of H-cement. Fireclay sand was chosen in two fractions to achieve the ideal workability of the mortar. During the production of the samples for the bending tests, no significant compaction was used on the vibratory bench. Compaction was applied only during the filling of the forms. Vibrating the forms of the protected sheets would have resulted in the deflection of the sheet, and thus in uncertainty about the required thickness of the H-cement protective layer.

2.2 Lightweight H-cement mortar
In order to achieve the lowest possible thermal conductivity, expanded perlite was used as a filler. Expanded perlite, with a low bulk density and excellent thermal properties, is ideal as an additive for thermal insulation mixtures. However, it is brittle, which significantly affects the process of making mixtures with H-cement. If the mixture is mixed for a long time or is not mixed gently, the expanded perlite is crushed into smaller particles (Šulc *et al.*, 2022). The formulation was determined with a water/binder ratio of 0.77, and the Stachement 508 plasticizer was chosen. The increase in the values of the water coefficients of the mixture is due to the use of expanded perlite as a very porous material. With sensitive mixing, and when the correct consistency of the mixture was found that avoided crushing the expanded perlite, a bulk density of 587 kg/m^3 was achieved in the wet state. This wet bulk density was similar to that of industrial fire plaster (Gravit *et al.*, 2022; Kiran *et al.*, 2022).

The knowledge gained from the first manufacturability tests indicated that a suitable ratio between H-cement and expanded perlite was 1:4.

Based on experience from previous mixing tests, a mixing machine was used for mixing the cement paste, and the required amount of expanded perlite was mixed into the paste with high sensitivity by hand. The recipe for lightweight H-cement mortar with expanded perlite is given in Table 4.

2.3 Samples for a fire experiment
For the experiment and to determine whether an expanded perlite-protected H-cement layer can protect steel structures at elevated temperatures, samples of 180 × 100 × 12 mm steel plate protected by a layer of H-cement mortar were chosen; see Figures 1–3. The dimensions
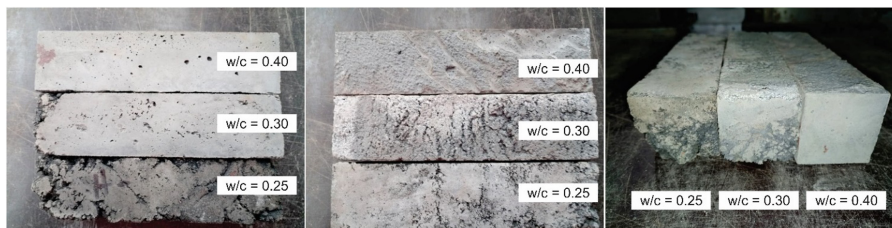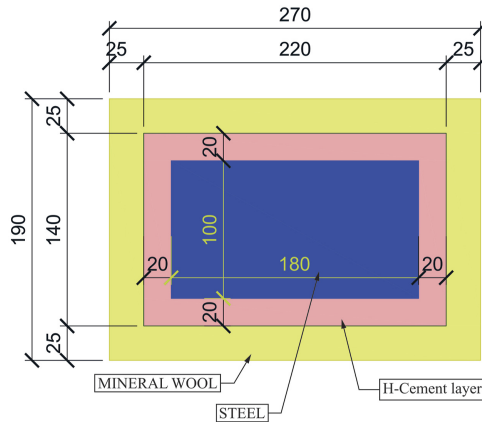

Source(s): Author's own creation

were determined based on the need to place four samples in a small-scale furnace during a single test. Any oil coating of the steel plate was removed, it was not provided with an adhesive bridge applied by the paint. To increase the adhesion of the protective layers to the steel sheet, the surface was covered with a paste less than 2 mm in thickness. Before filling, each form was oiled with a debonding emulsion, with increased emphasis on maintaining the surface cleanliness of the steel elements for ideal adhesion of the protective layer to the steel sheet. The height required to fill the protective layer was marked around the entire inner

	Specifications	Weight [kg]
H-cement	–	282
water	–	217
Stachema Plasticizer		4.3
Expanded perlite	0–1 mm	36
	1–2 mm	47
Source(s): Author's own creation		

Table 4.
Recipe for lightweight H-cement mortar with expanded perlite for 1 m^3

Figure 2.
Geometry of a sample and the position of the thermocouples

Source(s): Author's own creation

Figure 3.
Prepared samples – H-cement, fireclay sand, PVA fibres (all)

Source(s): Author's own creation

perimeter of the manufactured formwork to facilitate adherence to the required layer. For the fire experiment, the specimens were then insulated with mineral wool to enforce 1D heat conduction.

H-cement readily transitions to the ceramic phase (Martauz *et al.*, 2016), with only a relatively small shrinkage of the sample. Thermal conductivity of 0.12 W/m/K was assumed for H-cement.

Based on our pilot simulation and using sensitivity analysis, the thickness of the cement layer was determined to be 20 mm for a steel temperature criterion of 650 C. When investigating the temperature development for the temperature criteria and for the calculated protective layer thicknesses, the results were compared with the temperature development for the unprotected cross-section. For the experiment, 45 min of fire exposure was considered. The thickness of the necessary layer of the H-cement mixture was found to be 21.82 mm. To consider the error when constant properties of the protective layer are used, the calculated required depth was rounded to a thickness of 20 mm.

A calculation through the Arrhenius equation of the hydration heat demand was used to accelerate the maturity of the samples. The samples were stored at 32 C. The procedure for increasing the temperature for concrete maturation and decreasing the time for maturity has been discussed in (Kada-Benameur *et al.*, 2000). The time required for hydrating the specimens was calculated from these findings. Storing the samples at 32 C reduces the hydration time to 14 days.

The samples were treated against excessive evaporation of moisture during storage. Before the samples were placed in the drying furnace, they were cleaned of surface moisture, transported and measured. The temperature for drying the samples was set at 40 C to maintain the stability of the aluminates contained in the H-cement. The samples were reweighed at intervals of 2–3 days to observe the gradual weight loss due to the drying of the samples. The criterion for stopping the drying of the samples was set at a weight loss of <1% by weight in two consecutive weightings. The samples were dried for 9 days.

In order to assess the strengths of the H-cement mixtures for use in future experiments and for the development of the mixtures, the samples were tested on an MTS machine C43.304 for flexural strength and for compressive strength, according to the test standards. The MTS blast machine set was used as the standard procedure for loading the specimens in bending and in compression. Initial tests of ready-mixed mixtures tested by Martauz *et al.* (2016) were used to compare the strengths. For unmodified concrete formulations with H-cement binder without the need for increased fire resistance, similar mixes showed properties similar to those of CEM 32.5 R. During the loading process of the mixes, the fracturing was distinctly audible, and the cracking in the tested samples was also clearly visible. For lightweight mixtures, the fracture point was only visible when subtracted from the loading graph. Cracks due to the porosity of the samples were difficult to identify. Compression tests were performed on fractured parts, whereby the samples were loaded onto an MTS tearing machine with an attachment for compression testing of $40 \times 40 \times 40$ mm test cubes.

The loading process was carried out according to standard procedures in terms of a transverse displacement of 0.02 mm per second. The measured values are shown in Table 5.

3. Fire experiment
In addition to the fire experiment investigating the performance of the passive protection of H-cement, previous experiments have been done to investigate the behaviour of the material at higher temperatures. The first tests of this new H-cement were done by Daxner (2016) with a vermiculite filler. The basic characteristics were tested. Subsequently, adhesion tests were carried out with the concrete mix breaking away test to concrete (ASTM C1583) and to steel (ASTM E736). Additionally, carbonation tests, which are still pending (EN 12390–12),

accelerated chloride penetration tests (NT BUILD 443), permeability tests to chloride by migration test (ASTM C 1202), corrosion tests of steel reinforcement inside concrete (ASTM G109) and testing of the ability of machine spraying on structural surfaces. Results from the fire passive coating test are presented in this paper. Other parts of the experiments have been published or are still being tested.

3.1 Description of the test furnace

The basic requirements for the design of a fire test furnace are defined in EN 1363–1 ("EN 1363–1", 2020). The furnace is designed to obtain results according to the standard temperature curve (ISO 834–10:2014, 2014) of scaled samples and to predict the behavior of real structures. The small-scale test furnace has dimensions of $1.2 \times 0.8 \times 0.8$ m. The dimensions are based on the spatial arrangement of the room corner test on a reduced scale.

The furnace is heated by a gas burner with dimensions of $0.3 \times 0.1 \times 0.1$ m. The burner is in the middle of the furnace floor. Propane is used as the fuel. Thermocouples of type MTC10/1xK T2/P1,5/N3000/K-MM are placed evenly in the furnace. In the upper thermocouples, located 0.2 m below the ceiling of the test furnace, temperatures corresponding to the standard temperature curve are achieved. The scheme of the test furnace is shown in Figures 4 and 5.

The following requirements were met in the final placement of the samples in the furnace: the distance of the sample from the furnace wall is 100 mm, and the sample is placed 600 mm above the floor of the furnace.

	Flexular strength [MPa]	Compressive strength [MPa]
H-cement, fire clay, PVA fibres	8.35 ± 0.54	–
H-cement, expanded perlite	0.32 ± 0.07	0.61 ± 0.14
Source(s): Author's own creation'		

Table 5.
Strengths of the samples
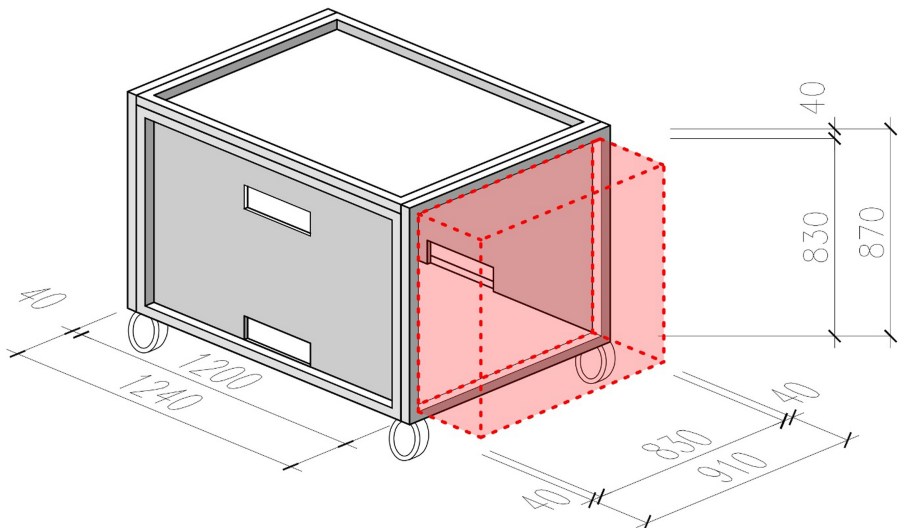
Figure 4.
Experimental small-scale furnace – axonometry

Source(s): Author's own creation
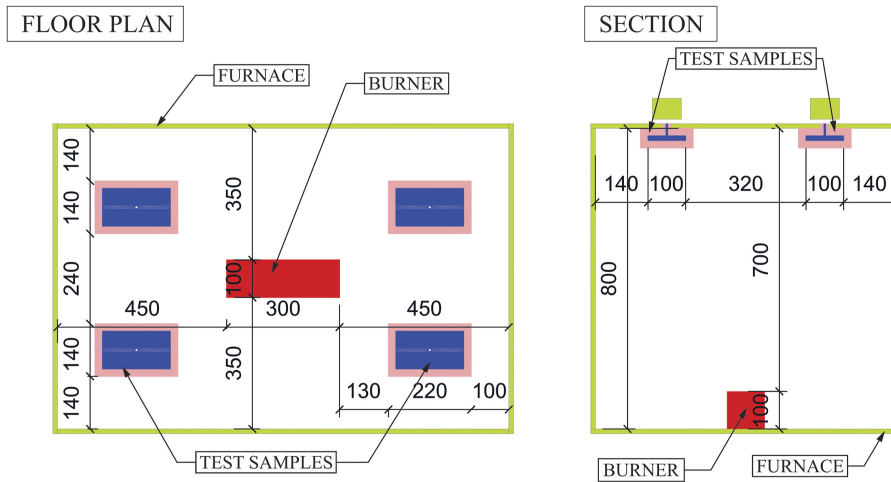
FLOOR PLAN

SECTION

Source(s): Author's own creation

3.2 Description of the fire experiment

The purpose of the experiments was to verify the effect of the protective layer, the insulation properties of the fire protection layer made of normal mortar with an H-cement binder, and the lightweight mortar made of H-cement. ISO 9705 standard ("ISO 9705–1:2016 Reaction To Fire Tests–Room Corner Test For Wall And Ceiling Lining Products–Part 1: Test Method For A Small Room Configuration", 2016) was followed for determining the temperature behavior in the small-scale furnace. The power setting of the burner placed in the furnace was used in accordance with previous experiments, e.g. Šejna (2021), Šejna *et al.* (2023a, b). Before the experiment, the samples were insulated with 25 mm thick mineral wool on the sides and from the top. The underside of the sample was exposed; see Figure 6.

Two MTC10/1xK T2/P1,5/N3000/K-MM thermocouples were placed on each tested sample in the long-axis direction. The distance between the thermocouples was 60 mm. The choice of location was appropriate for subsequently determining the heat transfer based on the finite element (FE) model.

Source(s): Author's own creation

The samples were transported to the FireLAB laboratory of UCEEB CTU 24 h before the experiments started. Each sample was heated for a similar period of 45 min and then the cooling phase temperatures were recorded for 15 min. The test furnace was placed under the exhaust bell, where the regulation of the amount of smoke and heat removed from the furnace was again controlled systemically. The fan power was set to 30% in the first phase of heating the samples in the furnace and was increased to 60% of its rated power in the more advanced phase. The position of the samples on the ceiling of the test furnace and the position of the burner are shown in Figure 7.

3.3 Temperature during the experiments

During the experiments, the following heat flow in the test furnace was observed. Higher temperatures were achieved in one part of the furnace than on the opposite side. This phenomenon was the same for all experiments; no measures were taken to adjust the boundary conditions in the test furnace. The different heating of the samples was used to investigate the different behavior of the elements under different heating. The more loaded elements were subjected to a temperature of approximately 900 C, and the less heated elements were subjected to a temperature of approximately 800 C.

The heating procedure for the lightweight layer experiment and the normal layer was identical, the standard temperature curve was followed. The temperatures measured in the fire protection layer H-cement with fireclay are shown in Figure 8. In the experiment, the fuel supply to the burner became unstable at 30 min and the temperatures in the furnace dropped. It was assessed that this decrease did not invalidate the test. For possible data evaluation, one sample was slightly moistened to measure the effect of water evaporation in the concrete. Figure 8 shows the effect of humidity on TC-07, when the heating of this sample was suspended at 100 C. Samples exposed to the same furnace temperature reached the same steel plate temperatures. The experiment is considered a success. An experiment with a lightweight protective layer is presented in Figure 9, when samples in the furnace were exposed to different temperatures. A standard temperature curve was followed for possible measures of the evolution of steel plate temperatures under the protective layer. During the experiment, temperatures up to 980 C were measured in the furnace. The temperature of the steel plate in the fire test did not exceed 400 C. The temperatures of the samples strained by the same temperature showed very small temperature differences, the experiment was again successful.
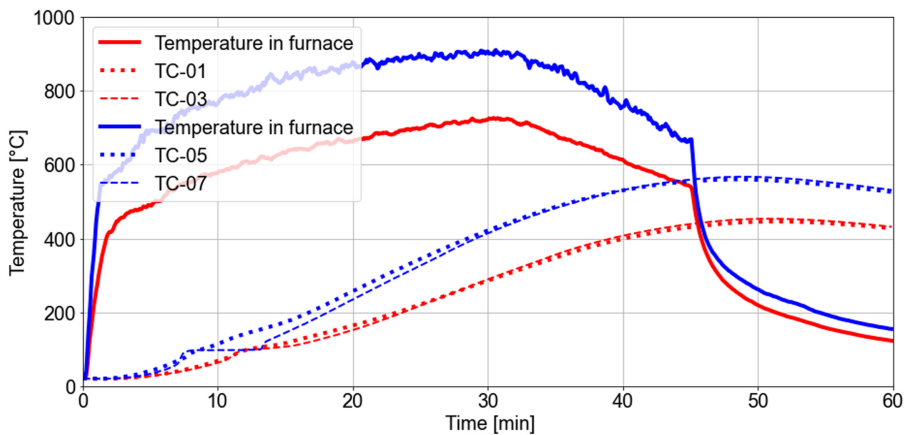
A comparison of the temperatures of the two experiments is shown in Figure 10. It is noticeable that the development of temperatures in both experiments was similar to the

Figure 7.
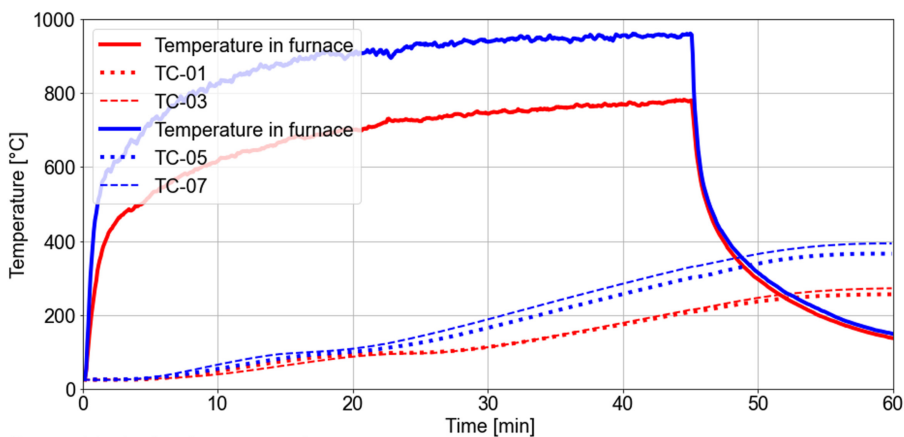Position of samples under the ceiling, and the position of the burner

Source(s): Author's own creation

Source(s): Author's own creation

Figure 8.
Temperature in
furnace and steel
plates, H-cement
mortar from
fireclay sand

Source(s): Author's own creation

Figure 9.
Temperature in
furnace and steel
plates, lightweight
H-cement mortar

30 min experiment. From the temperatures of the steel members, the lightweight protective layer reduces the heat transfer more significantly.

In the initial comparison of all samples immediately after removal from the test furnace onto the mineral wool boards, see Figure 11, the lightweight fire protective layer of the sample showed microscopic cracks in one-third of the length of the test element, see Figure 12. Compared to the lightweight variants, the fire protection layer of normal mortar was separated from the steel plate due to the different cooling of the steel and concrete. Better insulation properties of the unheated H-cement variant in comparison with the prediction were therefore demonstrated. Lightweight mixtures of H-cement with expanded perlite showed temperatures on the unprotected side of the steel of 330 C in the 45 min test. The proportion of PVA fibres added had no significant effect on the increase in resistance of the tested elements. The handling of the samples after cooling resulted in significant crumbling of the H-cement layer with expanded perlite.
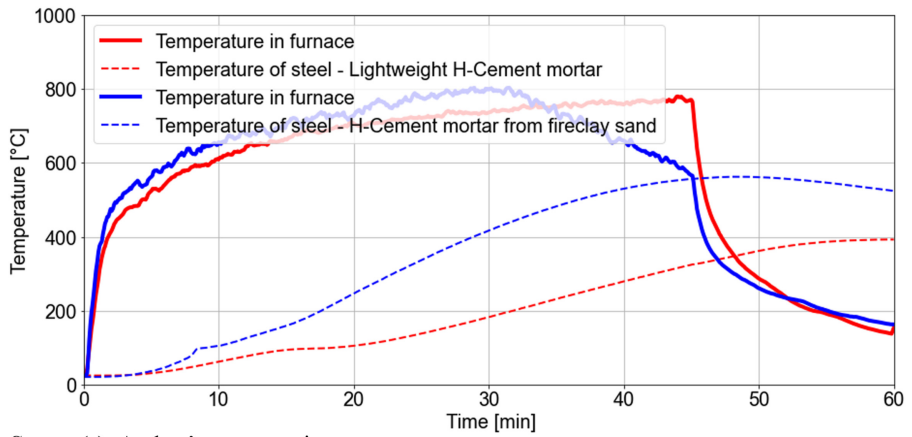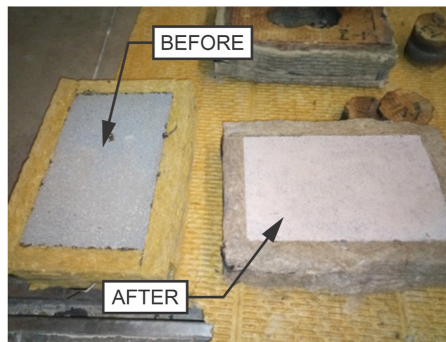
Source(s): Author's own creation
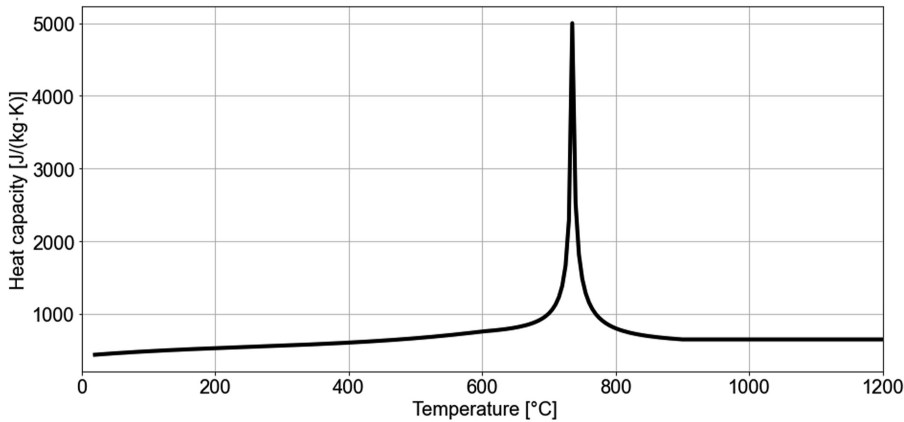
Source(s): Author's own creation

Source(s): Author's own creation

4. Determining the thermal conductivity of the Fire protective layer, using a numerical model
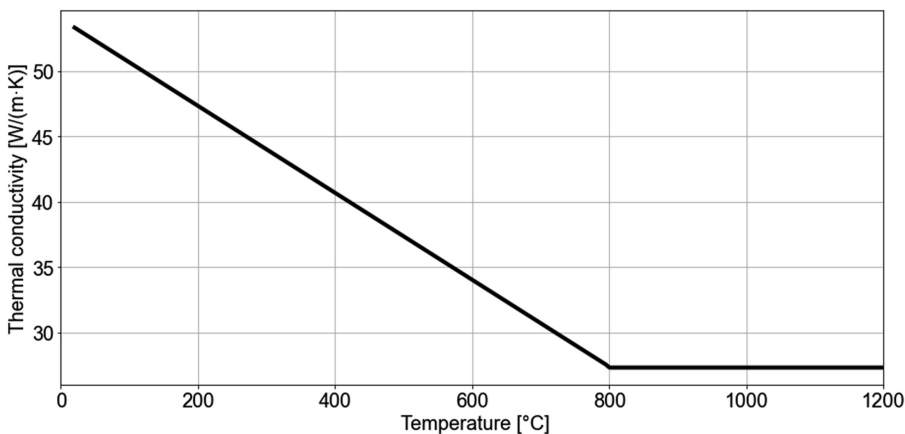
4.1 Numerical model

An FE model was developed to compare the temperatures measured by thermocouples on the unheated side of the steel with the thermal conductivity of the H-cement mortar. ANSYS mechanical software and thermal module (Stolarski *et al.*, 2019) were used. The geometry of the modelled sample corresponded to the experiments. The material characteristics of the steel element were taken from (Li and Wang, 2013). The material properties were considered as properties determined on the basis of the experiments. The dependence of the thermal conductivity and of the specific heat on temperature is shown in Figures 13 and 14.

The FE model was developed on the basis of knowledge acquired from previous research (Šejna, 2021) A hybrid computational mesh was chosen; for each layer, a minimum of 10 elements for steel were chosen throughout the width with set refinement during the transition between layers, and the tetrahedral element was used. A comparison of the four MESH

Source(s): Author's own creation

Figure 13.
Development of the
heat capacity of
the steel

Source(s): Author's own creation

Figure 14.
Development of the
thermal conductivity of
the steel

models is shown in Table 6 and the final MESH is shown in Figure 15. The development of the temperature distribution within the samples in numerical simulation is shown in Figure 16 for the lightweight H-cement mortar protective layer model.

By comparing the temperatures measured by the thermocouples on the unheated side of the steel with the FE models, a difference of 30 °C was observed after 60 min. In the initial

	MESHNo.1	MESHNo.2	MESHNo.3	MESHNo.4
Nodes	13,906	8,559	406,685	853,063
Elements	2,458	3,098	281,036	221,042
Type of MESH	Hexagonal	Tetrahedrons	Tetrahedrons	Hex dominant method
Calculation time	8 h[*)]	7 h[*)]	3 days[*)]	7 days[*)]

Table 6.
Development of the MESH numerical model

Note(s): [*)]Intel (R) Xeon (R) Gold 6144 CPU @3.50 GHz; socket: 16; virtual processor: 32; RAM 20 GB
Source(s): Author's own creation
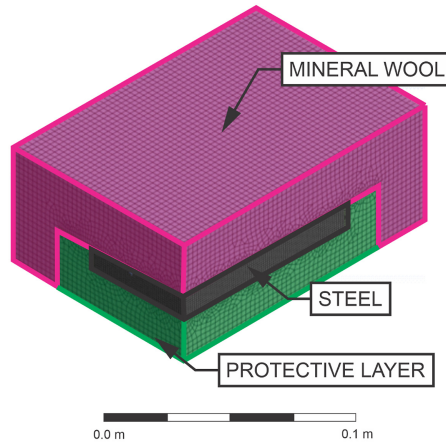
Figure 15.
MESH of the FE model

Source(s): Author's own creation
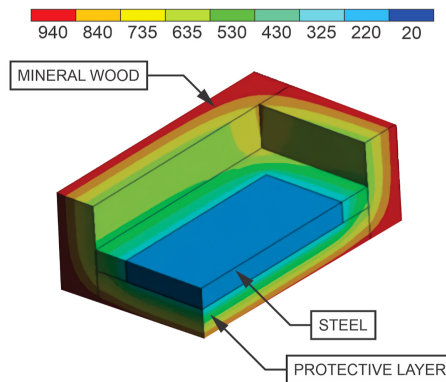
Figure 16.
Distribution of temperature in the samples
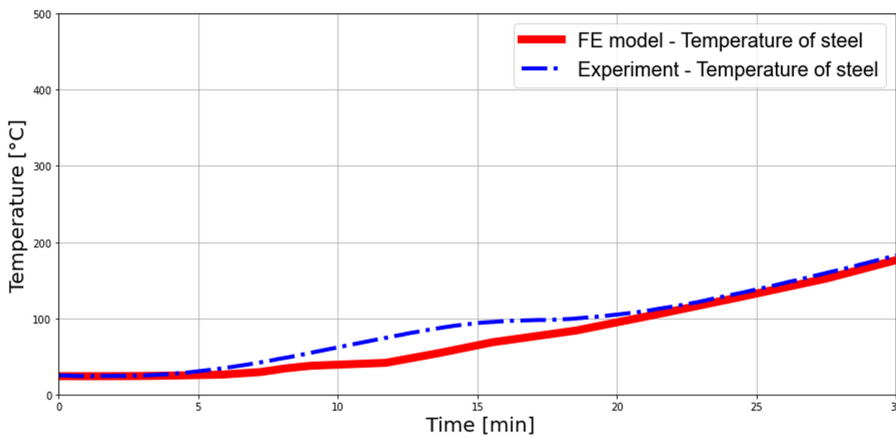
Source(s): Author's own creation

phases, the temperatures were identical. The progression is shown in Figures 17 and 18. For subsequent investigations of the protective layer, samples were taken from the TGA test method to determine the thermal properties of the mortar under investigation.

After adjusting the FE models to the thicknesses of the protective layer of lightweight H-cement mortar with expanded perlite, the temperatures were compared, considering constant thermal conductivity as predicted and according to the determined thermal conductivity depent temperature. The comparison is shown in Table 7 for thicknesses of 10, 15, 20 and 25 mm. For comparison, the standard temperature curve was used in the calculation.

4.2 Determining the thermal conductivity
When modelling the heat transfer to a given structure, it is necessary to take into consideration the methods that are used. Incorrect approaches to calculating the heat transfer

Source(s): Author's own creation

Figure 17.
Comparison of the temperature evolution in the FE model and in the experiment – normal H-cement mortar with fireclay sand and PVA fibres
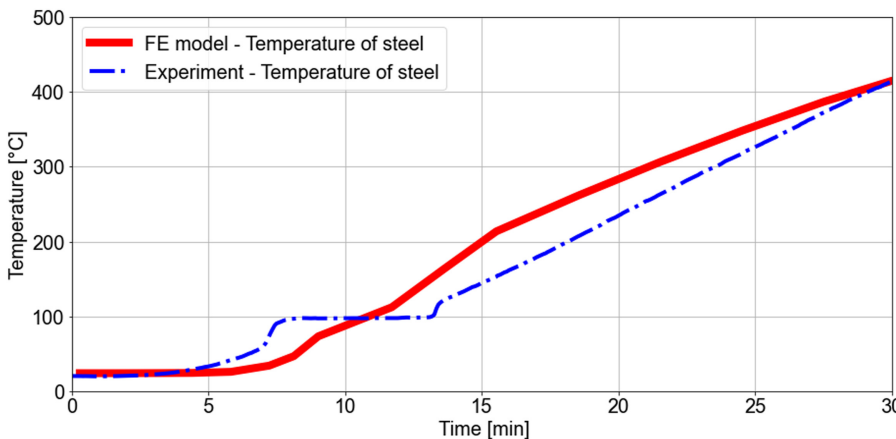
Source(s): Author's own creation

Figure 18.
Comparison of the temperature evolution in the FE model and in the experiment – lightweight H-cement mortar with expanded perlite

to a part of a structure can lead to the collapse of structures. In the event of a fire, the temperatures in the fire compartment rise very quickly. Accurate results corresponding to experiments are achieved by using the thermal dependent properties of the material. The findings of Wang *et al.* (2013) were used for predicting the material properties of lightweight H-cement with expanded perlite. However, in many cases, no values for describing the material were available. A prediction equation which can be applied in these cases (1), was, therefore, used to describe the thermal conductivity behavior of the porous H-cement material with expanded perlite.

$$\lambda = C_1 + C_2 T^3 \tag{1}$$

Coefficient C_1 expresses the thermal conductivity of the protective material at 20 C. Based on the experimental measurements, the A factor given (2) was adjusted upward to 0.29 in comparison with 0.27 for the vermiculite filler. The resulting equation for thermal conductivity at 20 C is given in (2), according to Wang *et al.* (2013). In small-scale furnace experiments, the thermal conductivity at 20 °C was found to be 0.117 W/m^2 for a bulk density of 487 kg/m^3.

$$C_1 = \lambda_0 = A \frac{\rho}{1000} = 0.29 \frac{\rho}{1000} \tag{2}$$

On the basis of experimental measurements, the thermal conductivity values of the fire protection layer made of H-cement and expanded perlite with a density of 487 kg/m^3 were determined by inverse analysis. The resulting values are given in Table 8, and the time history of the values is shown in Figure 19.

CTC = constant thermal conductivity; TDTC = temperature dependent thermal conductivity		15 min	30 min	45 min
10 mm	CTC	92.2℃	310.7℃	541.1℃
	TDTC	77.3℃	250.5℃	448.3℃
15 mm	CTC	61.0℃	218.1℃	417.1℃
	TDTC	52.9℃	174.7℃	335.5℃
20 mm	CTC	44.4℃	162.4℃	330.6℃
	TDTC	40.1℃	130.9℃	262.3℃
25 mm	CTC	34.5℃	125.4℃	267.3℃
	TDTC	32.3℃	102.3℃	211.2℃
Source(s): Author's own creation				

Table 7. Comparison of constant and temperature-dependent thermal conductivity temperatures

Density [kg/m^3]		487
Heat capacity [J/kg/K]		1150
Thermal conductivity [W/m/K]	20℃	0.12
	100℃	0.12
	200℃	0.12
	300℃	0.12
	400℃	0.12
	500℃	0.13
	600℃	0.14
	700℃	0.15
Source(s): Author's own creation		
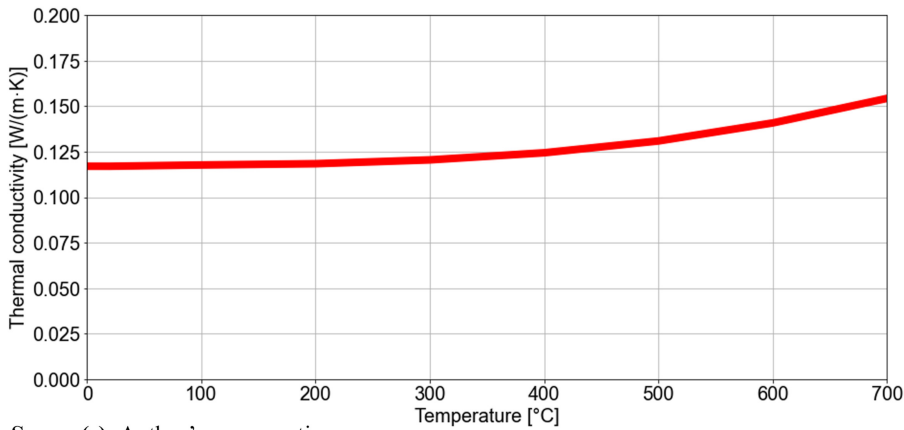
Table 8. Material properties of H-cement with expanded perlite

Source(s): Author's own creation

A lower value was found than the original assumption of the thermal conductivity of the mixture of H-cement and expanded perlite (0.12 W/(m·K) at 20 C). The improved thermal conductivity can be attributed to the effect of drying of the sample.
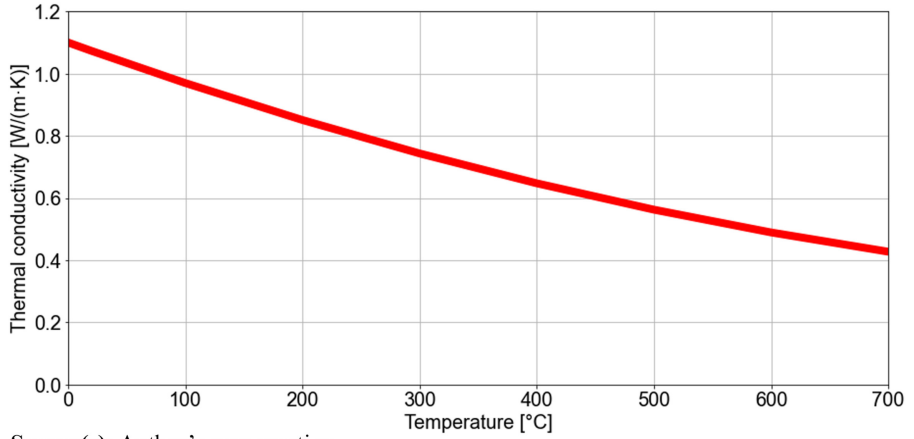
The effect of temperature on the change in bulk density and specific heat capacity was neglected for small samples. The change in the density of the protective materials is due to the evaporation of the moisture contained in the test samples. The samples were dried in a drying furnace, and the weight loss due to the evaporation of bound water in the samples was measured. The drying was stopped when the weight loss after two measurements was less than 1% of the previous weight. For the H-cement sample with expanded perlite, the final weight loss was 0.06%. Constant values were taken for the basic models for concrete with perlite filler. These values correspond to the volumetric weight of H-cement with expanded perlite.

The thermal conductivity of the protective layer of H-cement with fireclay sand and PVA fibres was calculated from the values measured in the experiment according to ("EN 13381–4:2013 Test methods for determining the contribution to the fire resistance of structural members Applied passive protection products to steel members, ISBN 978 0 580 77454 6", 2013). The development of the thermal conductivity of H-cement mortar from fireclay sand was determined from the measured data according to Equation (3). The resulting equation for the thermal conductivity of the fire protection layer of H-cement with fireclay sand and PVA fibres is given in (4). The resulting values are shown in Table 9 and the progression of the values is shown in Figure 20.

Density [kg/m^3]		1930
Heat capacity [J/kg/K]		1050
Thermal conductivity [W/m/K]	20℃	1.07
	100℃	0.97
	200℃	0.85
	300℃	0.74
	400℃	0.65
	500℃	0.56
	600℃	0.49
	700℃	0.43

Source(s): Author's own creation

Source(s): Author's own creation

$$\lambda_p = \left[d_p \frac{V}{A_p} C_s \rho_s (1 + \varnothing/3) \frac{1}{(T_{fi} - T_s)\Delta t} \right] \left[\Delta T_s + \left(e^{\varnothing/10} - 1 \right) \Delta T_{fi} \right] \tag{3}$$

$$\lambda_p = 1, 1 - 0, 136 \times 10^{-2} T + 0,0057 \times 10^{-4} T^2 \tag{4}$$

5. Conclusions

Experiments were conducted on the behaviour of the fire protection layer with an alkali-activated cement known as H-cement. The experiments followed the results and methods from small-scale sub-experiments already performed in which the properties of H-cement mortar, such as adhesion to steel and concrete surfaces, and the applicability of alkali-activated cement for fire protection applications were investigated. The findings regarding the possible use of passive protection were summarized in the introduction. For the experiments carried out, samples were tested in a small-scale furnace. The experiments took 45 min for heating and 15 min for cooling. There were two mortars, a lightweight H-cement mortar and a mortar made of H-cement and fireclay sand as filler. Experiments were conducted to determine the possible thermal conductivity of the two protective layers. The test samples in the furnace were exposed to different temperatures, so it was possible to determine the behaviour of the protective layers in more detail. In the numerical part of the research, FE models were developed for subsequent validation of the analytical determination of the thermal conductivity of the two fire protection layers. For the FE models, ANSYS mechanical with thermal analysis was used. The models confirmed the maximum deviation of 30°C. The determined thermal conductivity evolution for the H-cement lightweight mortar and the H-cement mortar with fireclay sand were presented.

For future research, it is necessary to focus on investigating the behavior of the passive protective layer on large-scale members, especially those under compressive stress, to confirm adhesion and prevent the debonding of the layer from the protected sample. Results from ongoing tests will be published.

The conclusions can be summarized as follows.

(1) Results from previous experiments have been confirmed.

(2) Using normal H-cement mortar with fireclay sand and PVA fibres, a ratio of 0.40 is suitable. For lightweight mortar with expanded perlite, a w/b ratio of 0.77 is suitable.

(3) The flexural strength of normal H-cement mortar with fireclay sand and PVA fibres was 8.35 ± 0.54 MPa, the flexural strength of the lightweight H-cement mortar with expanded was 0.32 ± 0.07 MPa

(4) The temperature-dependent thermal conductivity values were verified by FE models, which were compared with the experimental values.

(5) Hybrid alkali-activated cement (H-cement) is suitable for use as fire protection layers in steel structures; the specific heat waveform needs to be determined by TGA, and the performance of the protective layers needs to be verified by large-scale experiments.

(6) The use of hybrid cements, known as H-Cements, is very suitable for use for fire protection layers in steel structures, this protective layer resists high temperatures in a fire.

(7) To improve the sustainability of steel structures when fire loads increase, it is advisable to use lightweight H-Cement mortars to increase fire resistance. There is no significant additional load on the steel elements under a large increase in fire resistance.

References

Babrauskas, V. (2005), "Charring rate of wood as a tool for fire investigations", *Fire Safety Journal*, Vol. 40 No. 6, pp. 528-554, doi: 10.1016/j.firesaf.2005.05.006.

Buchanan, A.H. and Abu, A.K. (2017), *Structural Design for Fire Safety*, 2nd ed., John Wiley & Sons, West Sussex, ISBN: 978-0-470-97289-2.

Damrongwiriyanupap, N., Srikhamma, T., Plongkrathok, C., Phoo-ngernkham, T., Sae-Long, W., Hanjitsuwan, S., Sukontasukkul, P., Li, L. and Chindaprasirt, P. (2022), "Assessment of equivalent substrate stiffness and mechanical properties of sustainable alkali-activated concrete containing recycled concrete aggregate", *Case Studies in Construction Materials*, Vol. 16, doi: 10.1016/j.cscm.2022.e00982.

Daxner, J. (2016), "Use of hybrid cement in fireresistant plasters", pp. 1-8, (882016), available at: doi: 10.1021/acs.analchem.5b04814

Gravit, M., Shabunina, D., Antonov, S. and Danilov, A. (2022), "Thermal characteristics of fireproof plaster compositions in exposure to various regimes of fire", *Buildings*, Vol. 12 No. 5, doi: 10.3390/buildings12050630.

Hlaváček, P., Šmilauer, V., Škvára, F., Kopecký, L. and Šulc, R. (2015), "Inorganic foams made from alkali-activated fly ash: mechanical, chemical and physical properties", *Journal of the European Ceramic Society*, Vol. 35 No. 2, pp. 703-709, doi: 10.1016/j.jeurceramsoc.2014.08.024.

ISO 834-10:2014 (2014), *ISO 834-10:2014 Fire Resistance Tests - Elements of Building Construction - Part 10: Specific Requirements to Determine the Contribution of Applied Fire Protection Materials to Structural Steel Elements*, International Organization for Standardization.

Jani, P. and Imqam, A. (2021), "Class C fly ash-based alkali activated cement as a potential alternative cement for CO2 storage applications", *Journal of Petroleum Science and Engineering*, Vol. 201, doi: 10.3390/ma15103437.

Jogl, M., Koťátková, J. and Reiterman, P. (2016a), "Differences in the mechanical properties of lightweight refractory cementitious composites reinforced by various types of fibers", *Key Engineering Materials*, Vol. 677, pp. 29-32, doi: 10.4028/www.scientific.net/KEM.677.29.

Jogl, M., Reiterman, P., Holčapek, O., Koťátková, J. and Konvalinka, P. (2016b), "Residual properties of fiber-reinforced refractory composites with a fireclay filler", *Acta Polytechnica*, Vol. 56 No. 1, pp. 27-32, doi: 10.14311/APP.2016.56.0027.

Kada-Benameur, H., Wirquin, E. and Duthoit, B. (2000), "Determination of apparent activation energy of concrete by isothermal calorimetry", *Cement and Concrete Research*, Vol. 30 No. 2, pp. 301-305, doi: 10.1016/S0008-8846(99)00250-1.

Kim, S. and Kim, S. (2020), "Framework for designing sustainable structures through steel beam reuse", *Sustainability*, Vol. 12 No. 22, doi: 10.3390/su12229494.

Kiran, T., Yadav, S., N, A., Mathews, M., Andrushia, D., lubloy, E. and Kodur, V. (2022), "Performance evaluation of lightweight insulating plaster for enhancing the fire endurance of high strength structural concrete", *Journal of Building Engineering*, Vol. 57, doi: 10.1016/j.jobe.2022.104902.

Lennon, T. and Moore, D. (2003), "The natural fire safety concept—full-scale tests at Cardington", *Fire Safety Journal*, Vol. 38 No. 7, pp. 623-643, doi: 10.1016/S0379-7112(03)00028-6.

Li, G. and Wang, P. (2013), "Properties of Steel at Elevated Temperatures", *Advanced Analysis and Design for Fire Safety of Steel Structures*, Springer, Berlin, pp. 37-65, doi: 10.1007/978-3-642-34393-3_3.

Martauz, P., Janotka, I., Strigáč, J. and Bačuvčík, M. (2016), "Fundamental properties of industrial hybrid cement: utilization in ready-mixed concretes and shrinkage-reducing applications", *Materiales de Construcción*, Vol. 2016 No. 66322, p. 84.

Mirshekarlou, B., Budayan, C., Dikmen, I. and Birgonul, M. (2021), "Development of a knowledge-based tool for waste management of prefabricated steel structure projects", *Journal of Cleaner Production*, Vol. 323, doi: 10.1016/j.jclepro.2021.129140.

Mizukami, T. and Tanaka, T. (2017), "Determination of design fire load for structural fire safety in the compartment subdivided by non-fire-rated partitions", in Harada, K., Matsuyama, K., Himoto, K., Nakamura, Y. and Wakatsuki, K. (Eds), *Fire Science and Technology 2015*, Springer, Singapore, doi: 10.1007/978-981-10-0376-9_34.

Nan, Z., Khan, A., Jiang, L., Chen, S. and Usmani, A. (2022), "Application of travelling behaviour models for thermal responses in large compartment fires", *Fire Safety Journal*, Vol. 134, doi: 10.1016/j.firesaf.2022.103702.

Ozaki, F., Tezuka, K. and Mori, Y. (2018), "Estimation on failure probability of a steel member at fully-developed compartment fire", *Journal of Structural and Construction Engineering (Transactions of AIJ)*, Vol. 83 No. 753, pp. 1725-1733, doi: 10.3130/aijs.83.1725.

Rangwala, A. and Raghavan, V. (2022), *Compartment Fires*, Mechanism of Fires, Springer, Berlin, pp. 177-196, doi: 10.1007/978-3-030-75498-3_7.

Šejna, J. (2021), "Small furnace experiments for wood burning pyrolysis models", *Civil Engineering Research Journal*, Vol. 12 No. 3, pp. 1-11, doi: 10.19080/CERJ.2021.12.555838.

Šejna, J., Dobrovolný, P. and Wald, F. (2023a), "The partial fire protection of steel members: a comparative study", *Journal of Structural Fire Engineering*, Vol. ahead-of-print No. ahead-of-print, doi: 10.1108/JSFE-01-2023-0001.

Šejna, J., Šulc, S. and Wald, F. (2023b), "Fire protection of steel and concrete structures by alkali-activated cement – adhesion and fire experiment", *Architecture and Sustainable Development*, CTU FCE, Vol. 22, pp. 123-132.

Shi, C., Krivenko, P. and Roy, D. (2006), "Alkali-activated cements and concretes".

Siebers, R., Hauke, B., Helmus, M. and Meins-Becker, A. (2017), "Sustainability considerations for the construction phase of steel structures", *Ce/Papers*, Vol. 1 Nos 2-3, pp. 4630-4639, doi: 10.1002/cepa.524.

Stolarski, T., Nakasone, Y., Yoshimoto, S. and Winter, W. (2019), "Engineering analysis with ANSYS software", *Applied Mechanics and Materials*, Vol. 887, pp. 21-29, doi: 10.1016/C2016-0-01966-6.

Šulc, S., Šejna, J., Šmilauer, V. and Wald, F. (2022), "Steel elements with timber fire protection - experiment and numerical analysis", *Acta Polytechnica CTU Proceedings*, Vol. 34, doi: 10.14311/APP.2022.34.0116.

Šulc, S., Šmilauer, V., Šejna, J. and Wald, F. (2021), "Fire protection of steel elements using lightweight hybrid cement mortar", *Acta Polytechnica CTU Proceedings*, Vol. 30 No. 20, pp. 104-108, doi: 10.14311/APP.2021.30.0104.

Wang, Y., Burgess, I. and Wald, F. (2013), *Performance-based Fire Engineering of Structures*, 2012 ed., CRC Press.

Wang, H., Wang, L., Shen, W., Cao, K., Sun, L., Wang, P. and Cui, L. (2022), "Compressive strength, hydration and pore structure of alkali-activated slag mortars integrating with recycled concrete powder as binders", *KSCE Journal of Civil Engineering*, Vol. 26 No. 2, pp. 795-805, doi: 10.1007/s12205-021-0406-1.

Further reading

EN 1363-1:2020 (2020), "Fire resistance tests - Part 1: General requirements", *International Organization for Standardization*.

EN 13381-4:2013 (2013), Test methods for determining the contribution to the fire resistance of structural members applied passive protection products to steel members, *International Organization for Standardization*, ISBN 978 0 580 77454 6.

ISO 9705-1:2016 (2016), *Reaction to Fire Tests - Room Corner Test for Wall and Ceiling Lining Products - Part 1: Test Method for A Small Room Configuration*, International Organization for Standardization.

Corresponding author
Jakub Šejna can be contacted at: jakub.sejna@fsv.cvut.cz